Journal of Nano- and Electronic Physics
Vol. **16** No 2, 02001(6pp) (2024)

Журнал нано- та електронної фізики
Том **16** № 2, 02001(6cc) (2024)

OPEN ACCESS

REGULAR ARTICLE

Effect of Introduction Layers of Native Oxide, InN, and InSb on the Electrical Characterization of the Au/*n*-InP

Ali Sadoun* ✉

Applied Materials Laboratory, Research Center (CFTE), Sidi Bel Abbès Djillali Liabes University, 22000, Algeria

(Received 15 December 2023; revised manuscript received 17 April 2024; published online 29 April 2024)

Our study examined how native oxide layers, InN and InSb, affected the current-voltage and capacitance-voltage characteristics of the Au/*n*-InP Schottky diode at a temperature of 300 K with and without interface states, traps, and tunneling current. The simulation was carried out using the Atlas-Silvaco-Tcad device simulator. From our results, we found that the effective barrier heights were measured to be 0.474 eV, 0.544 eV, and 0.561 eV via *I-V* measurements and 0.675 eV, 0.817 eV, and 0.80 eV via *C-V* measurements. Additionally, we utilized the high-low frequency method to calculate the average density of interface state density, which was determined to be approximately $6.03 \cdot 10^{11}$ and $3.33 \cdot 10^{12}$ cm $^{-2} \cdot$ eV $^{-1}$. The results indicate that a thin film of InN and InSb can effectively passivate the InP surface, as evidenced by the good performance of the passivized sample.

Keywords: InP, InN, InSb, Schottky diodes, Current–Voltage, Capacitance–Voltage, Interface state density.

DOI: 10.21272/jnep.16(2).02001 PACS numbers: 00.11.Al, 00.11.Sa

1. INTRODUCTION

Indium nitride (InN) is a semiconductor material that is made up of indium (In) and nitrogen (N) atoms. It has a wide band gap of around 0.7 eV [1, 2], which makes it suitable for high-temperature and high-power applications. InN is also a direct band gap semiconductor, which means that its energy band gap is directly proportional to the energy difference between the valence and conduction bands. This property makes it useful for optoelectronics, such as UV and blue light-emitting diodes (LEDs) and laser diodes [3]. InN is also used in high-frequency and high-power electronic devices, such as (HEMTs) and Schottky diodes. Additionally, InN is a good material for high-frequency and high-power electronic devices, as it have high electron mobility and a high electron saturation velocity. [4]

Indium antimonide (InSb) is a semiconductor material that is made up of indium (In) and antimony (Sb) atoms. It has a narrow band gap of around 0.17 eV [1], which makes it a suitable material for detection in the infrared spectrum. InSb is an indirect band gap semiconductor, which means that its energy band gap is not directly proportional to the energy difference between the valence and conduction bands. This property makes it useful for infrared detectors and other optoelectronics applications. [5]

InSb has very high electron mobility, it is used in high-frequency and high-speed electronic devices like HEMT, FET, HBT, and others. It also has a very high electron saturation velocity, making it a good choice for high-frequency and high-power electronic devices. [6, 7]

Au/InN/InP and Au/InSb/InP are both heterostructures consisting of three layers: a layer of gold (Au) on top, a middle layer of either indium nitride (InN) or indium antimonide (InSb), and a bottom layer of indium phosphide (InP).

Many research groups investigated *n*-InP-based metal-semiconductor by using different contact schemes, for instance, B. Hadjadj et all [8] reported Fabrication and electrical characterization of thin films obtained by the nitridation of InP (100) substrates in a Glow Discharge Source are presented and discussed. A. Fritah et all [9] carried out an analysis of electronic parameters of Au/n-InP by the simulation of I–V–T and C–V–T characteristics. A. Fritah et all [10] performed analysis of electronic parameters Characteristics of Au/*n*-InP at Low Temperature. A.H. Khediri et all [11] performed an analysis of the electrical properties of Au/InN/*n*-InP and obtained a value of barrier height (0.64 eV). The samples were produced using a glow discharge technique in an ultra-high vacuum environment. A. Sadoun et all [7] performed an analysis of the electrical properties Schottky diode in the temperature range (300 K to 425 K) and obtained a value of barrier height are 0.602 to 0.69 eV, respectively.

In this article, we will perform an analysis of the current-voltage characteristics for the simulated near-ideal diode, real diode, Au/InN/*n*-InP, and Au/InSb/InP structures at T = 300 K. We will use the computer program we have developed in the form of helper and complementary subroutines for the Atlas Silvaco software. This study is dedicated to the determination of electrical parameters such as the potential barrier, ideality factor, and series resistance using various methods (V-I, Mikhelashvili, and C-V). We will present the effect of native oxide layers, InN and InSb on the current-voltage characteristics of the Au/*n*-InP struc-

* Correspondence e-mail: ali.sadoun@dl.univ-sba.dz

Cite this article as: Ali Sadoun, *J. Nano- Electron. Phys.* 16 No 2, 02001 (2024) https://doi.org/10.21272/jnep.16(2).02001

ture. The structure used in the simulation is based on experimental work [11, 12] to compare our results.

2. DEVICE STRUCTURE

In this study, we are using a reference structure that we will study (by simulation) a Schottky diode made on an n-type InP substrate. The metal contact was formed with gold (Au), as shown in Fig. 1. In this study, we use an n-type epitaxial layer with an approximate thickness of 0.7 μm doped with a donor concentration of 5×10^{16} cm $^{-3}$, and an n^+ substrate of 300 μm thickness doped with a concentration of 1×10^{19} cm $^{-3}$, a thin film of native oxide of about 5 Å and layers of InN and InSb of about 20 Å was created on the top of the substrate n-type InP.

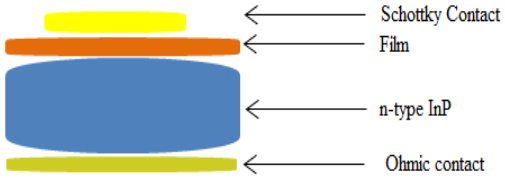

Fig. 1 – Schematic of simulation Au/Film/n-InP

3. THE SIMULATION

A simulation was run using Atlas-Silvaco-Tcad, a tool that offers comprehensive simulation capabilities for the electrical, optical, and thermal behavior of semiconductor devices in 2D and 3D, based on physical principles used: [13, 14]

- Band gap model and Universal Schottky tunneling
- Shockley–Read–Hall model and Mobility model
- Auger recombination, Impact ionization, and thermionic emission

Table 1 gives the physical, electrical, and technological parameters of InN, InP, and InSb used in the simulation.

4. RESULT AND DISCUSSIONS

4.1 Current-Voltage (*I-V*) Method

Introducing InN or InSb layers on the InP surface can modify the interface properties due to the difference in the band alignment and the interface chemistry. I-V measurements can be used to study the rectification behavior and the barrier height of the interface, which can be influenced by the type and thickness of the introduced layer.

The graph in Fig. 2 shows the current-voltage measurement taken at a temperature of 300 K. I-V characteristics may be described by (1) [7, 22, 23].

$$I = I_0 \left[1 - \exp\left(\frac{q(V-IR)}{nkT}\right)\right] \quad (1)$$

where I_0, n, T, and k are the saturation current, the ideality factor, the temperature in Kelvin, and the Boltzmann constant. The saturation current I_0 is expressed by [14]:

$$I_0 = AT^2A^* \exp\left(\frac{q\Phi_{b0}}{kT}\right) \quad (2)$$

where A and A^* are the contact area and the effective Richardson constant, q and Φ_{b0} are the electron charge and the barrier height. The values of the Richardson constant ($A^* = 9.4$ A/cm^2 K^2 for n-InP [12]).

The values of the diode's parameters, such as the ideality factor, forward voltage drop, and reverse leakage current, can be extracted from the experimental data using various analysis techniques. First, we proceed with the (I-V) method the Fig. 2 shows the current-voltage characteristics I(V) of the near ideal diode and real diode at temperature 300 K, on a semi-logarithmic scale. In forward bias, the log I(V) curve has two parts, the first linear part between 0 and 0.3 V, and a second part beyond 0.3 V which shows a curvature due to the influence of the series resistance.

Table 1 – InN, InP, and InSb parameters.

	InN	**InP**	**InSb**
N_C (cm $^{-3}$)	$4.6 \cdot 10^{17}$ [15]	$5 \cdot 10^{17}$ [16]	$3.28 \cdot 10^{16}$ [17]
N_V (cm $^{-3}$)	$2.7 \cdot 10^{19}$ [15]	$2 \cdot 10^{19}$ [16]	$3.7 \cdot 10^{18}$ [18]
ε_r	10.5 [19]	12.1 [16]	15.9 [17]
χ (eV)	5.8 [19]	4.38 [16]	4.59 [17]
μ_n (cm^2/V.s)	4000 [2]	4500 [16]	70000 [17]
μ_p (cm^2/V.s)	39 [19]	100 [16]	750 [20]
E_g (eV)	0.7 [21]	1.35 [16]	0.17 [17]

The ideality factor can be extracted from the slope of the linear region in the *log*(I)-V plot at low forward bias voltages. The slope is equal to the inverse of the ideality factor, which can be used to estimate the quality of the interface and the recombination mechanisms at play.

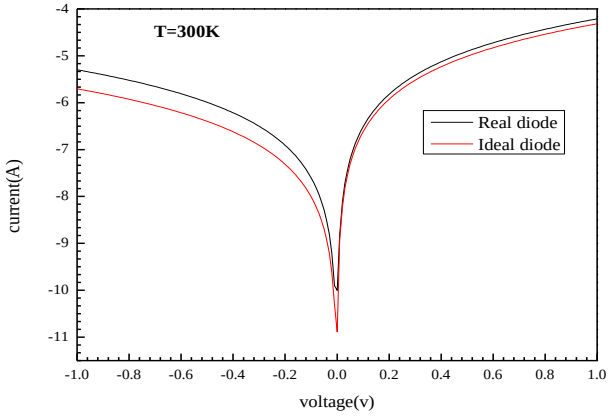

Fig. 2 – The simulated semi-logarithmic current-voltage characteristic of the near ideal diode and real diode at temperature 300 K

From Fig. 2 and Eq. 2, the calculated value of the barrier height, ideality factor, and series resistance are (0.385 eV; 1.056, and 15.83 Ohms) for a near ideal diode.

To study the real diode, we employed a thin native oxide layer with a thickness of 5 angstroms and a permittivity of 7.9 [24]. The positive charge between the n-InP semiconductor and the oxide layer was [25]. We used tunneling current (universal Schottky tunneling model [9]) for the transport mechanism and four deep acceptor traps and acquired experimental results. The value of the barrier height, ideality factor, and series resistance are (0.474; 1.122, and 27.27 Ohms). The difference between an Ideal diode and a Real diode in electronic properties is the native oxide layer's formation due to surface contaminants such as oxygen and carbon impurities.

Fig. 3 depicts the I-V characteristics of the simulated Au/InN/*n*-InP and Au/InSb/InP at 300 K temperature in a semi-logarithmic scale. There is a noticeable high leakage current, which can be attributed to the small barrier height and the temperature's influence on the reverse saturation current. Table 2 presents the calculated values of the barrier height and the ideality factor as a function of temperature. It can be seen that the barrier height values increase for both Au/InN/*n*-InP and Au/InSb/InP.

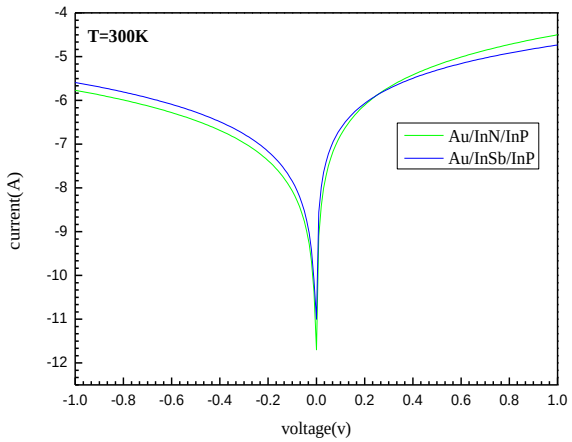

Fig. 3 – Semi-logarithmic scale current-voltage characteristic of the Au/InN/*n*-InP and Au/InSb/InP at temperature 300 K

4.2 Mikhelashvili Method

Mikhelashvili's method is another way to determine the electrical parameters [26].

This method is based on equation (3):

$$\theta(v) = \frac{d(\ln(I))}{d(\ln(v))} \tag{3}$$

the electrical parameters can be calculated from the following relation (4),(5), and (6): [27]

$$n = \frac{qv_m(\theta_m - 1)}{kT\theta_m^2} \tag{4}$$

$$\Phi_b = \frac{kT}{q}\left[\theta_m + 1 - \ln\left(\frac{I_m}{AA^*T^2}\right)\right] \tag{5}$$

$$R_s = \frac{v_m}{I_m\theta_m^2} \tag{6}$$

Here (θ_m and V_m) are the coordinates of the maximum point in θ (V) vs. V plot.

Fig. 4 shows the obtained Mikhelashvili plots for the real diode, Au/InN/*n*-InP, and Au/InSb/InP. We have determinate values of the electrical parameters are presented in Table 2.

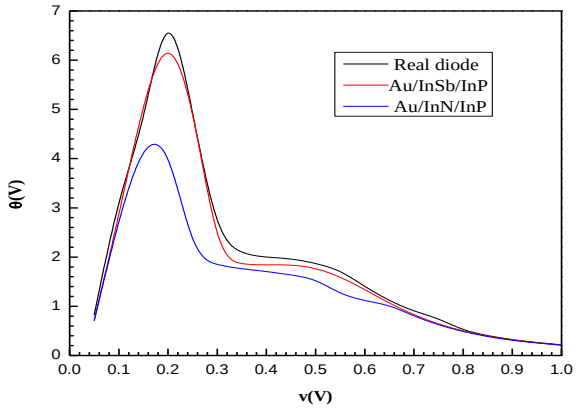

Fig. 4 – Mikhelashvili's plots for the real diode, Au/InN/*n*-InP, and Au/InSb/InP at temperature 300 K

4.3 Chattopadhyay Model

Chattopadhyay's method [28] can be used to calculate the electrical parameters from the Ψ_s (V) behavior shown in Fig. 5. The barrier height is determined using an equation (7):

$$\Phi_b = \Psi_s(J_C, V_C) + C_2V_C + V_n - \frac{kT}{q} \tag{7}$$

where, $\Psi s, V_C$ presents the critical surface potential, the critical voltage. The critical surface potential value can be calculated from the following relation (8) [28, 29]:

$$\Psi_s = \frac{kT}{q}\ln\left(\frac{AA^*}{I}\right) - v_n \tag{8}$$

And V_n, C_2 parameters can be determined by relation (9), (10) : [28, 30]:

$$v_n = \frac{kT}{q}\ln\left(\frac{N_c}{N_d}\right) \tag{9}$$

$$C_2 = \frac{1}{n} = \left(\frac{d\Psi_s}{dV}\right)_{Jc,v_c} \tag{10}$$

Fig. 5 shows the surface potential-forward voltage curves ($\Psi_s - V$) of the real diode, Au/InN/*n*-InP, and Au/InSb/InP structures for temperature 300 K. The results obtained $\Psi_s(J_C, V_c)$, and the electrical parameters, are shown in Table 2.

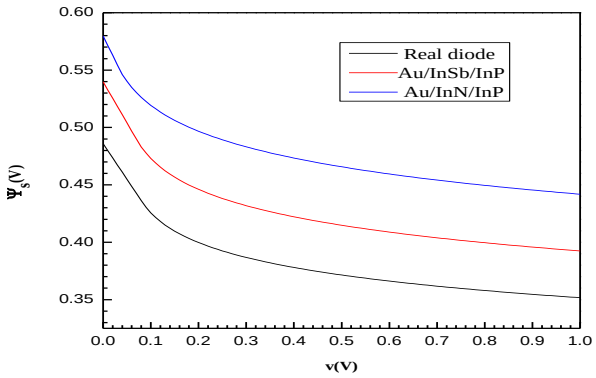

Fig. 5 – The surface potential- voltage curves of the real diode, Au/InN/*n*-InP and Au/InSb/InP at temperature 300 K

4.4 Capacitance-Voltage Characteristics

Capacitance-voltage (C-V) characteristics are a type of measurement used to study the electrical properties of diodes. The measurement involves applying an alternating voltage signal to the device and measuring the resulting capacitance as a function of the applied voltage.

Fig. 6 displays the simulated reverse bias C $^{-2}$ – V plot at a frequency of 1 MHz for a temperature of 300 K. The inset shows the capacitance across the entire reverse bias range and the depletion layer capacitance is indicated as:

$$\frac{1}{C^2} = \frac{2(V_R+V_d)}{q\varepsilon_s N_D A^2} \quad (11)$$

Where V_R and V_d are the voltage in the reverse bias and the diffusion potential, ε_s = 12.1 and ε_0 = 8.85 × 10 $^{-14}$ F/cm the permittivity of the semiconductor, and the vacuum dielectric constant respectively, and N_D is the doping concentration. The barrier height is defined by [16]:

$$\Phi_{bn} = V_d + \frac{kT}{q} + V_n \quad (12)$$

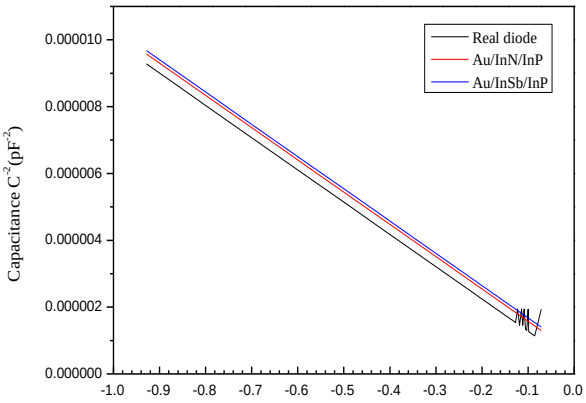

Fig. 6 – The simulated C-V characteristic of the real diode, Au/InN/*n*-InP and Au/InSb/InP at temperature 300 K

Table 2 groups the different parameters extracted from semi-logarithmic scale current–voltage characteristic of the real diode, Au/InN/*n*-InP and Au/InSb/InP structures using the different methods at the temperature 300 K.

Table 2 – The obtained values of electrical parameters for Au /InP, Au/InN/*n*-InP, and Au/InSb/InP in T = 300 K

From	Parameters	Real Diode	Au/InN/InP	Au/InSb/InP
(I-V) characteristics	Barrier height	0.474	0.544	0.561
	Ideality factor	1.122	1.583	1.621
	Series resistance	27.27	40.25	47.08
C-V	Barrier height	0.675	0.817	0.802
Mikhelashvili's method	Barrier height	0.623	0.681	0.692
	Series resistance	33.8	43.2	48.1
Chattopadhyay's method	Barrier height	0.545	0.605	0.644
	Ideality factor,	1. 42	1.52	1.60
	surface potential	0.391	0.424	0.463

We employed multiple techniques, including conventional forward bias I-V, C-V, Chattopadhyay, and Mikhelashvili, to determine the ideality factor, barrier height, and series resistance. The results showed that the inclusion of the InN and InSb insulating layer improved the diode's performance by raising the barrier height. 0.474 eV to 0544 eV and the layer of InSb 0.474 to 0561 from I-V measurements and 0.675 to 0.817 eV and 0.675 to 0.802 eV from C-V measurements.

The cleaning of the InP substrate surface with ionic bombardment eliminated surface contaminants like oxygen and carbon, leading to a lower interface state density. The nitridation process also improved the interfacial crystallographic defects by forming an InP layer. This outcome is consistent with the high concentration of defects found in nitride materials and matches results from other studies on GaAs substrates. These findings emphasize the crucial role of interface states in the current flow in electronic devices and the importance of keeping them as low as possible to reduce surface recombination and tunneling.

The InN and InSb layer deposited on InP is amorphous because it has not undergone annealing, and the band gap for InN is 0.7 eV and InSb is 0.17 eV. For these reasons, the dominant current in our structure is thermionic from a Schottky contact. However, The current in the structure can be influenced by various factors such as the type of semiconductor material, the nature of the metal-semiconductor interface, and the presence of any impurities or defects in the device. In general, the current in a metal-semiconductor junction can be due to a combination of thermionic emission, tunneling, and recombination processes. The dominant mechanism depends on various parameters such as the barrier height, doping density, and temperature.

The variations in the barrier height values obtained from the methods could be a result of the data being extracted from different parts of the forward-bias I-V plot. The values obtained are similar to those found by Akkal et al. [31] on Au/InSb/InP (100) Schottky diode and A.H. Khediri [11] on Au/InN/InP Schottky diode.

4.5 Determination of Interface States Density (Nss)

To determine the density of the interface state distribution [11].by low frequencies, all of the interface states follow the AC signal, the capacitance at low frequencies can be expressed [32]:

$$C_{LF} = \frac{\sqrt{q\varepsilon_s N_D/2\psi_s} + qN_{ss}}{1+qJR_s/kT + \delta/\varepsilon_i\left(\sqrt{q\varepsilon_s N_D/2\psi_s} + qN_{ss}\right)} \quad (13)$$

where N_{SS} and δ are the interface state density, and the

thickness of the interfacial layer, respectively.

And high frequency can be expressed[32] :

$$C_{HF} = \frac{\sqrt{q\varepsilon_s N_D / 2\psi_s}}{1 + qJR_s/kT + \delta/\varepsilon_i \sqrt{q\varepsilon_s N_D / 2\psi_s}} \quad (14)$$

The interface state density N_{SS} can be determined using Eqs. (13) and (14), such as :[33]

$$N_{ss} \approx \sqrt{q\varepsilon_s N_D / 2\psi_s} \frac{C_{LF} - C_{HF}}{qC_{HF}} \quad (15)$$

In n-type semiconductors, the energy of the interface states relative to the top of the conduction band (E_C-E_{SS}) at the semiconductor surface can be expressed: [34]

$$E_c - E_{ss} = q(\Phi_{bn} - V) \quad (16)$$

After (C-V) measurements end Eqs (16), it is possible to determine the interface state density for the two structures Au/InN/n-InP and Au/InSb/InP based solely on the given statement. The temperature-dependent variation of the interface states in the forbidden band was determined and illustrated in Fig. 7.

From this curve, we then read values of the interface state density at order $6.03 \cdot 10^{11}$ and $3.33 \cdot 10^{12}$ cm $^{-2}$.eV $^{-1}$ for two structures Au/InN/n-InP and Au/InSb/InP

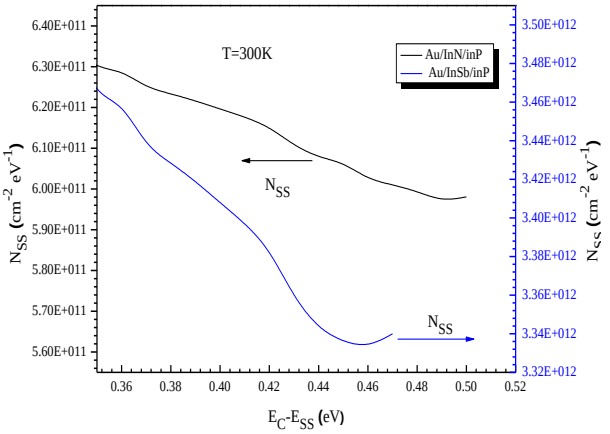

Fig. 7 – Interface state density energy distributions of Au/InN/n-InP and Au/InSb/InP diode by L-H Frequency C-V

5. CONCLUSION

In this paper, the electrical characteristics of the Au /InP, Au/InN/n-InP, and Au/InSb/InP structures were analyzed. The results showed that the I-V and C-V curves of the diode were affected by the InN and InSb layers, leading to increase barrier heights and low density of interface states. The effective barrier heights were found to be 0.474, 0544, and 0.561 eV from I-V measurements and 0675, 0.817 and 0.802 eV from C-V measurements. Compared to conventional Au/n-InP Schottky diodes, the prepared Au/InN/n-InP and Au/InSb/InP Schottky diode showed improved characteristics due to the passivation of the InP surface with an interfacial InN and InSb layers, which reduced the density of interface states

REFERENCES

1. Thermal properties of the group III nitrides, INSPEC, 1998.
2. V. Kumar, D.R. Roy, *J. Mater. Sci.* **53**, 8302 (2018).
3. G.D. Chern, E.D. Readinger, H. Shen, M. Wraback, C.S. Gallinat, G. Koblmüller, J.S. Speck, *Appl. Phys. Lett.* **89**, 141115 (2006).
4. G. Koblmüller, C. Gallinat, S. Bernardis, J. Speck, G. Chern, E. Readinger, H. Shen, M. Wraback, *Appl. Phys. Lett.* **89**, 071902 (2006).
5. B. Akkal, Z. Benamara, L. Bideux, B. Gruzza, *Microelectron. J.* **30**, 673 (1999).
6. Z. Benamara, B. Akkal, A. Talbi, B. Gruzza, L. Bideux, *Mater. Sci. Eng.: C* **21**, 287 (2002).
7. A. Sadoun, I. Kemerchou, *International Journal of Energetica (IJECA)* **5**, 31 (2020).
8. B. Hadjadj, Z. Benamara, N. Zougagh, B. Akkal, *Molec. Cryst. Liquid Cryst.* **627**, 74 (2016).
9. A. Fritah, A. Saadoune, L. Dehimi, B. Abay, *Philosoph. Mag.* **96**, 2009 (2016).
10. A. Fritah, L. Dehimi, F. Pezzimenti, A. Saadoune, B. Abay, *J. Electron. Mater.* 48, 3692 (2019).
11. A. Khediri, A. Talbi, M. Benamara, Z. Benamara, *J. Nano-Electron. Phys.* **13** No 4, 04002 (2021).
12. M. Soylu, B. Abay, *Microelectron. Eng.* **86** No 1, 88 (2009).
13. A.U.s.M. SILVACO-TCAD, Silvaco International, California (2004).
14. A. Sadoun, S. Mansouri, M. Chellali, N. Lakhdar, A. Hima, Z. Benamara, *Mater. Sci.-Poland* 37, 496 (2019).
15. M.E. Levinshtein, S.L. Rumyantsev, M.S. Shur, *Properties of Advanced Semiconductor Materials: GaN, AIN, InN, BN, SiC, SiGe* (John Wiley & Sons: 2001).
16. H. Mathieu, H. Fanet, *Physique des semiconducteurs et des composants électroniques-6ème édition: Cours et exercices corrigés* (Dunod: 2009).
17. S. Adachi, *Optical constants of crystalline and amorphous semiconductors: numerical data and graphical information* (Springer Science & Business Media: 2013).
18. H.D. Trinh, Y.C. Lin, E.Y. Chang, C.-T. Lee, S.-Y. Wang, H.Q. Nguyen, Y.S. Chiu, Q.H. Luc, H.-C. Chang, C.-H. Lin, *IEEE Trans. Electron Dev.* **60**, 1555 (2013).
19. Z. Fan, S. Mohammad, W. Kim, *Appl. Phys. Lett.* **68**, 1672 (1996).
20. S.N. Usmonov, A. Saidov, A.Y. Leiderman, *Phys. Solid State* **56**, 2401 (2014).
21. I. Vurgaftman, J.N. Meyer, *J. Appl. Phys.* **94**, 3675 (2003).
22. H. Dogan, S. Elagoz, *Physica E:* **63**, 186 (2014).
23. A. Sadoun, I. Kemerchou, S. Mansouri, M. Chellali, *Int. J. Energ.* **5**, 37 (2020).
24. H. Çetin, E. Ayyildiz, *Appl. Surf. Sci.* **253**, 5961 (2007).
25. H. Çetin, E. Ayyıldız, *Physica B: Condensed Matter* **394**, 93 (2007).
26. V. Mikhelashvili, G. Eisenstein, V. Garber, S. Fainleib, G. Bahir, D. Ritter, M. Orenstein, A. Peer, *J. Appl. Phys.* **85**, 6873 (1999).
27. A. Sadoun, S. Mansouri, M. Chellali, A. Hima, Z. Benamara, *2018 International Conference on Communications and Electrical Engineering (ICCEE), IEEE*, 1 (2018).
28. P. Chattopadhyay, *Solid-State Electron.* **38**, 739 (1995).

29. Ş. Karataş, N. Yildirim, A. Türüt, *Superlattice. Microst.* **64**, 483 (2013).
30. S. Ali, M. Sedik, C. Mohammed, L. Nacereddine, H. Abdelkader, B. Zineb, *Mater. Sci.-Poland* **38**, 165 (2020).
31. B. Akkal, Z. Benamara, N.B. Bouiadjra, S. Tizi, B. Gruzza, *Appl. Surf. Sci.* **253**, 1065 (2006).
32. B. Daouia, Analyse et conception des antennes microrubans alimentées par guide d'onde coplanaire, in: UNIVERSITE DE MOHAMED BOUDIAF M'SILA FACULTE DE TECHNOLOGIE (2016).
33. H. Unlu, N.J. Horing, J. Dabowski, *Low-dimensional and nanostructured materials and devices: properties, synthesis, characterization, modelling and applications* (*Springer*: 2016).
34. T.D. Veal, C.F. McConville, W.J. Schaff, *Indium Nitride and Related Alloys* (CRC press: 2011).

Вплив введених шарів природного оксиду, InN та InSb на електричні характеристики Au/*n*-InP

Ali Sadoun

Applied Materials Laboratory, Research Center (CFTE), Sidi Bel Abbès Djillali Liabes University, 22000, Algeria

У дослідженні було перевірено, як природні шари InN та InSb впливають на вольт-амперні та вольт-ємнісні характеристики діода Шотткі Au/*n*-InP при температурі 300 К з і без станів розділу, пасток і тунельного струму. Моделювання проводилося за допомогою симулятора пристрою Atlas-Silvaco-Tcad. На основі вольт-амперних характеристик було установлено, що ефективна висота бар'єрів становить 0,474; 0,544 і 0,561 еВ, на основі вольт-ємнісних характеристик – 0,675; 0,817 і 0,800 еВ. Крім того використання високо-низькочастотного методу для розрахунку середньої щільності міжфазних станів, яка була визначена приблизно як $6.03 \cdot 10^{11}$ and $3.33 \cdot 10^{12}$ см$^{-2} \cdot$ еВ$^{-1}$. Результати показують, що тонка плівка InN та InSb може ефективно пасивувати поверхню InP, про що свідчить висока продуктивність зразка.

Ключові слова: InP, InN, InSb, Діоди Шотткі, Вольт-амперна характеристика, Вольт-ємнісна характеристика, Інтерфейс, Щільність станів.